(^{3}He,t) reaction on the double β decay nucleus ^{48}Ca and the importance of nuclear matrix elements

E.-W. Grewe,[1] D. Frekers,[1] S. Rakers,[1,*] T. Adachi,[2,†] C. Bäumer,[1] N. T. Botha,[3] H. Dohmann,[1] H. Fujita,[4,5] Y. Fujita,[2] K. Hatanaka,[6] K. Nakanishi,[6,‡] A. Negret,[7,§] R. Neveling,[5] L. Popescu,[7,‖] Y. Sakemi,[6,¶] Y. Shimbara,[2,**] Y. Shimizu,[6,‡] F. D. Smit,[5] Y. Tameshige,[6] A. Tamii,[6] J. Thies,[1] P. von Brentano,[8] M. Yosoi,[9,††] and R. G. T. Zegers[10]

[1]*Institut für Kernphysik, Westfälische Wilhelms-Universität, D-48149 Münster, Germany*
[2]*Department of Physics, Osaka University, Toyonaka, Osaka 560-0043, Japan*
[3]*Department of Physics, University of Cape Town, Rondebosch 7700, South Africa*
[4]*School of Physics, University of the Witwatersrand, Johannesburg 2050, South Africa*
[5]*iThemba LABS, POB 722, Somerset West 7129, South Africa*
[6]*Research Center for Nuclear Physics, Osaka University, Ibaraki, Osaka 567-0047, Japan*
[7]*Vakgroep Subatomaire en Stralingfysica, Universiteit Gent, B-9000 Gent, Belgium*
[8]*Institut für Kernphysik, Universität zu Köln, D-50937 Köln, Germany*
[9]*Department of Physics, Kyoto University, Sakyo, Kyoto 606-8224, Japan*
[10]*National Superconducting Cyclotron Laboratory, The Joint Institute for Nuclear Astrophysics and the Department of Physics and Astronomy, Michigan State University, East Lansing, Michigan 48824, USA*

(Received 24 July 2007; published 8 November 2007)

High-resolution (^{3}He, t) measurements on the double β-decay ($\beta\beta$) nucleus ^{48}Ca have been performed at RCNP (Osaka, Japan) to determine Gamow-Teller (GT$^-$) transitions to the nucleus ^{48}Sc, which represents the intermediate nucleus in the second-order perturbative description of the $\beta\beta$ decay. At a bombarding energy of $E_{^3\mathrm{He}} = 420$ MeV an excitation energy resolution of 40 keV was achieved. The measurements were performed at two angle positions of the Grand Raiden Spectrometer (GRS): 0° and 2.5°. The results of both settings were combined to achieve angular distributions, by which the character of single transitions could be determined. To characterize the different multipoles, theoretical angular distributions for states with $J^\pi = 1^+, 2^+, 2^-$, and 3^+ were calculated using the distorted-wave Born approximation (DWBA) Code DW81. The GT$^-$ strength was extracted up to $E_x = 7$ MeV and combined with corresponding GT$^+$ strength deduced from the ^{48}Ti(d, ^{2}He)^{48}Sc data to calculate the low-energy part of the $\beta\beta$-decay matrix element for the ^{48}Ca $2\nu\beta\beta$ decay. We show that after applying trivial momentum corrections to the (^{3}He, t) spectrum, the two reaction probes, (p, n) and (^{3}He, t) reveal a spectral response to an impressively high degree of similarity in the region of low momentum transfer.

DOI: 10.1103/PhysRevC.76.054307 PACS number(s): 25.45.Kk, 25.55.−e, 23.40.Hc, 27.40.+z

I. INTRODUCTION

Charge-exchange reactions have been established to be useful probes for determining Gamow-Teller (GT) distributions in β^+ and β^- direction [1–4]. At intermediate energies and at forward angles, i.e., low-momentum transfers (i.e., $\Delta L = 0$), (n, p) and (p, n) reactions selectively excite GT transitions due to the dominance of the $V_{\sigma\tau}$ component of the effective interaction [4–7]. More recently, the (d, ^{2}He) reaction performed at KVI, Groningen (NL) [8,9], the (t, ^{3}He) reaction at MSU, Michigan (USA) [10] and the (^{3}He, t) reaction at RCNP, Osaka (JP) [11,12] have been established as high-resolution alternatives to the elementary (n, p) and (p, n) reactions. Resolutions on the order of 100 keV in the case of (d, ^{2}He), 190 keV for (t, ^{3}He), and 40 keV for (^{3}He, t) can routinely be achieved. High-resolution experiments are of key importance when extracting the $2\nu\beta\beta$-decay matrix element, as the present study will demonstrate.

The connection of the $2\nu\beta\beta$-matrix element with the decay rate for the $\beta\beta$ decay is given by:

$$\Gamma^{2\nu}_{(\beta^-\beta^-)} = G^{2\nu}(Q, Z)\left|M^{(2\nu)}_{\mathrm{DGT}}\right|^2, \tag{1}$$

where $G^{2\nu}(Q, Z)$ is a phase-space factor depending on the Q value of the reaction and the Z value of the decaying nucleus. Further, it contains the weak interaction coupling constant. The $2\nu\beta\beta$-decay matrix element can be deduced by combining GT$^+$ and GT$^-$ distributions in the following way [3]:

$$M^{(2\nu)}_{\mathrm{DGT}} = \sum_m \frac{\langle 0^{(f)}_{\mathrm{g.s.}}\| \sum_k \sigma_k\tau_k^- \| 1^+_m\rangle\langle 1^+_m \| \sum_k \sigma_k\tau_k^- \| 0^{(i)}_{\mathrm{g.s.}}\rangle}{1/2\, Q_{\beta\beta}\left[0^{(f)}_{\mathrm{g.s.}}\right] + E_x(1^+_m) - E_0} = \sum_m \frac{M_m^{GT^+}\cdot M_m^{GT^-}}{1/2\, Q_{\beta\beta}\left[0^{(f)}_{\mathrm{g.s.}}\right] + E_x(1^+_m) - E_0}. \tag{2}$$

---

*EADS Astrium Space Transportation GmbH, TE53 Avionics Engineering, 28199 Bremen, Germany.
†RCNP, Osaka University, Ibaraki, Osaka 567-0047, Japan.
‡CNS, University of Tokyo, RIKEN campus, Wako, Saitama 351-0198, Japan.
§European Commission, DG JRC, IRMM, B-2440 Geel, on leave of absence from NIPNE, Bucharest, Romania.
‖KVI, University of Groningen, NL-9747 AA Groningen.
¶CYRIC, Tohoku University, Aoba, Sendai, Miyagi 980-8578, Japan.
**Graduate School of Sciences and Technology, Niigata University, Nishi, Niigata 950-2181, Japan.
††RCNP, Osaka University, Ibaraki, Osaka 567-0047, Japan.

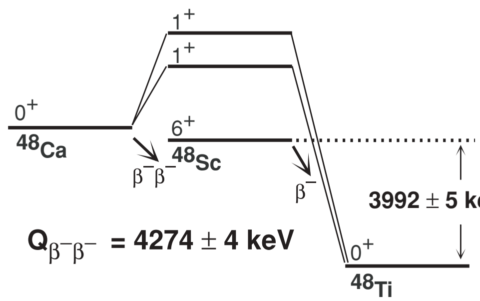

FIG. 1. Schematic representation of the $\beta\beta$ decay of ^{48}Ca [21]. The single β^- decay to the intermediate ^{48}Sc is forbidden by angular momentum.

Here, $E(1^+_m) - E_0$ is the energy difference between the m^{th} intermediate 1^+ state and the initial ground state, and the sum $\sum_k$ runs over all the neutrons of the decaying nucleus [13,14]. Contributions from Fermi type virtual transitions are negligible, because initial and final states belong to different isospin multiplets. In fact, the transition matrix is essentially a sum of products of two ordinary β-decay Gamow-Teller matrix elements between the initial and the intermediate states and between the intermediate states and the final ground state. Because in this case two real neutrinos are emitted, the intermediate states m that contribute will be 1^+ states, whose transition matrix elements can be determined, e.g., through charge-exchange reactions in the β^+ and β^- direction at intermediate energies of 100–200 MeV/nucleon [3,5,6,15–19] or, for the ground-state transitions, by measuring the single (β^+ / EC) and β^--decay rates [20]. The situation for ^{48}Ca is sketched in Fig. 1.

To establish a good correspondence between the levels as they are excited from the one and the other GT direction, good resolution is mandatory and the (n, p) and (p, n) elementary reaction experiments, although the cleanest, as far as the reaction mechanism is concerned, cannot easily provide this. Anderson *et al.* [19] have performed the (p, n) experiments at IUCF in 1985 with a resolution of about 360 keV, and at TRIUMF, where many leading (n, p) experiments were performed, the resolution for the reaction ^{48}Ti$(n, p)^{48}$Sc was about 1.3 MeV [3]. Recently, when the ^{48}Ti$(d, {}^2$He) reaction was used as an alternative to (n, p), it gave a remarkable insight into the details of the different excitation paths, showing that states excited strongly from one direction seemed to be only weakly excited from the other, which demonstrated impressively the importance of the nuclear structure entering theoretical estimates for calculating the $2\nu\beta\beta$-decay rate. These observations were unveiled as a direct consequence of the good resolution of about 100 keV.

In this report the (^{3}He, t) reaction on ^{48}Ca is being presented as a possible high-resolution alternative to the (p, n) reaction. We note, however, that the similarity of the two probes, i.e., (p, n) and (^{3}He, t), the latter being an entirely composite probe, has not yet fully been tested, and some recent studies do in fact give evidence of differences, at least in those cases where the GT strength is comparatively small [22–25]. The prospect of good resolution is nonetheless attractive, as it allows a much more detailed comparison with theoretical models and for the potential to give rather precise estimates for the $2\nu\beta\beta$-decay rate. Such a detailed comparison is highly warranted for many of the $\beta\beta$-decay nuclei, not only ^{48}Ca, as the understanding of the nuclear structure embedded in the $2\nu\beta\beta$-decay matrix elements is an important step toward a reliable estimate for the alternative $0\nu\beta\beta$-decay mode [26–28]. Although in this latter case the nuclear structure is significantly more complex, the knowledge of these matrix elements allows one to extract the neutrino mass, once the neutrinoless $\beta\beta$-decay mode is experimentally established [29–35].

II. EXPERIMENT

The experiment was performed at the Research Center for Nuclear Physics (RCNP) at Osaka University, Japan. The ^{3}He beam at 420 MeV was provided through the cascade acceleration with the $K = 120$ AVF cyclotron and the $K = 400$ RCNP Ring Cyclotron.

The beam transport consisted of the high-resolution "WS course" beamline [36]. Beamline and Grand Raiden Spectrometer (GRS) [37] are designed for high-resolution experiments and are equipped with several focusing units to improve the energy resolution. To achieve a high resolution, beam-matching techniques were employed [38]. The realization of matching conditions was examined by using the "faint beam method" [39,40]. Outgoing tritons were momentum analyzed in the GRS within its full acceptance of ±20 mrad in horizontal and ±40 mrad in vertical direction. The primary beam was stopped by a Faraday cup inside the first dipole magnet. Further details of the optics are described in Ref. [41].

The detection system consisted of a set of two vertical drift chambers (VDC), which allowed precise track reconstruction at the focal plane [42]. Behind the VDCs two thin (3- and 10-mm) plastic scintillators were placed for particle identification and trigger [43].

A thin 1.87-mg/cm^2 self-supporting ^{48}Ca target with an isotopic enrichment of 95.2% was used. Its thickness contributed to the final energy resolution to about 29 keV.

The spectra were momentum calibrated using a $^{\text{nat}}$MgO target, which provides numerous levels at well-known excitation energies distributed over a large portion of the focal plane, but also employing the three strongest and well-established transitions in ^{48}Sc at 2.53 MeV (1^+), 6.71 MeV (0^+), and 16.84 MeV (1^+). The accuracy of the absolute energy determination is about ±10 keV.

III. DETAILED ANALYSIS

A ^{48}Ca(^{3}He, t)^{48}Sc spectrum is shown in Fig. 2. Due to the excellent energy resolution of 40 keV (fwhm), the spectrum contains highly detailed information, which allows identification of many individual levels up to about 20 MeV excitation. At energies below about 8 MeV, two strong transitions dominate the spectrum, the GT transition at 2.53 MeV and the Fermi transition to the 0^+, $T = 4$ isobaric analog state (IAS) at 6.71 MeV. This observation is consistent with the one made by Anderson *et al.* [19] using the (p, n) reaction. Between 6 and 9 MeV lies a region of highly fragmented states, and at around 10 MeV one enters the

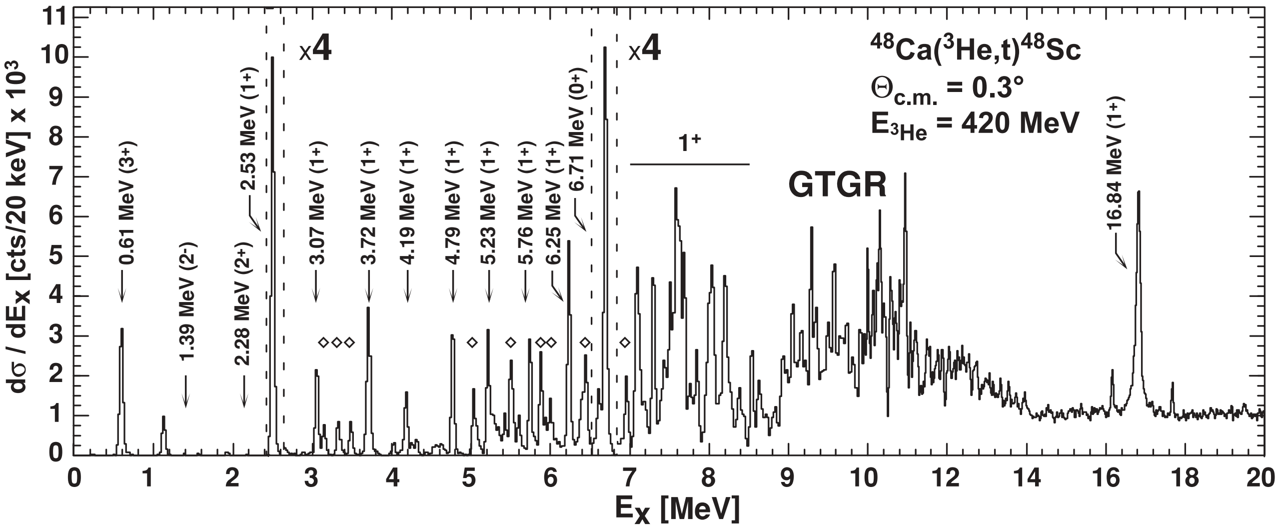

FIG. 2. Excitation energy spectrum of the ^{48}Sc final nucleus excited through the ^{48}Ca(^{3}He, t)^{48}Sc reaction at 420 MeV. The spectrum was taken at an GRS angle of 0°. Up to about 9 MeV single states can be identified. Note that above 10 MeV the energy scale is compressed. The levels at 2.53 MeV and 6.71 MeV are both scaled down by a factor of 4. Levels marked with a diamond (◇) are identified as weak, by some extent overlapped 1^+ transitions. At larger angles nearby higher multipole transitions dominate the angular distributions.

Gamow-Teller giant resonance (GTGR) regime, where most of the GT$^-$ strength resides. A complete analysis of the GTGR will be the subject of a separate publication. Above 13 MeV the spectrum is relatively flat, and at around 16.84 MeV one observes the transition to the 1^+, $T = 4$ state, which is analog to the 1^+ state in ^{48}Ca at 10.22 MeV [44].

To extract angular distributions, the data of both spectrometer settings (0° and 2.5°) were divided into five angle intervals $\Delta\Theta_{\rm scat} = [0°, 0.5°]$, $[0.5°, 1.0°]$, $[1.0°, 1.5°]$, $[1.5°, 2.0°]$, $[2.0°, 2.5°]$ and $\Delta\Theta_{\rm scat} = [1.5°, 2.0°]$, $[2.0°, 2.5°]$, $[2.5°, 3.0°]$, $[3.0°, 3.5°]$, $[3.5°, 3.6°]$. The last bin of the 2.5° setting of the GRS is at the angular acceptance limit and is accordingly small containing low statistics. The overlap regions of two sets of angle bins were used for solid angle cross-calibration to be insensitive to possible variations of the large dispersion on target. In Fig. 3 angular distributions are shown for selected strong J^π transitions, including the transitions to the two analog states at 6.71 MeV (IAS) and 16.84 MeV. The J^π values are known in all cases [21] and are confirmed by comparing the experimental with calculated angular distributions.

A. Distorted-wave-model calculations

The distorted-wave Born approximation code DW81 of Raynal and Comfort was used [45,46] for the reaction calculations. It calculates charge-exchange cross sections using microscopic transition densities based on shell-model wave functions and an effective interaction, whose structure is based on the approach of Love and Franey [47]. Distortion of incoming and outgoing waves is treated in an optical model. The single-particle wave functions were generated from Woods-Saxon potentials with a radius $r_0 = 1.25$ fm and a diffuseness parameter $a = 0.5$ fm [48]. The Coulomb radius was set to $r_c = 1.3$ fm and the Thomas spin-orbit strength to $\lambda = 25$ [49]. The single-particle occupation numbers were calculated using the shell-model code OXBASH [50] with the (pf) interaction of Kuo and Brown [51]. These were then input into NORMOD [52] calculations to determine the one-body transition densities (OBTD). In DW81 the effective projectile-target interaction is written in terms of Yukawa potentials (for a detailed discussion see Refs. [53,54]). The parameters of the different components of the effective ^{3}He nucleon force have been determined by the following procedure:

(i) The V_τ component was evaluated by comparing the calculation with the experimental angular distribution of the transition to the IAS (see Fig. 3). For this transition the central $\sigma\tau$ term and the tensor term do not contribute. Further, the LS component can safely be neglected [54], as it becomes important only for high-spin states of natural parity.

(ii) To determine the $V_{T\tau}$ component, one uses high-spin states of unnatural parity, as these are mediated by this interaction. Those states appear in the spectrum only as weakly excited states (here: 2^- and 3^+ states), which makes the determination difficult. When choosing the value for $V_{T\tau}$ given in Ref. [49], one arrives at a good agreement between theoretical and experimental angular distributions.

(iii) After identifying V_τ and $V_{T\tau}$, the central component $V_{\sigma\tau}$ is derived from the strongest 1^+ transition.

The ^{3}He optical model parameters were extracted from Ref. [55]. There are no optical model parameters for tritons available; therefore, potential depth parameters for the outgoing tritons were estimated to be 85% of those of ^{3}He following the recipe of Refs. [49,56].

In Fig. 3 the DW81 calculations for various J^π transitions are presented. The low-spin excitations are remarkably well reproduced, whereas deficiencies of the model seem to be getting more apparent for the higher spin states, like, e.g., the 2^+ and the 3^+ excitations.

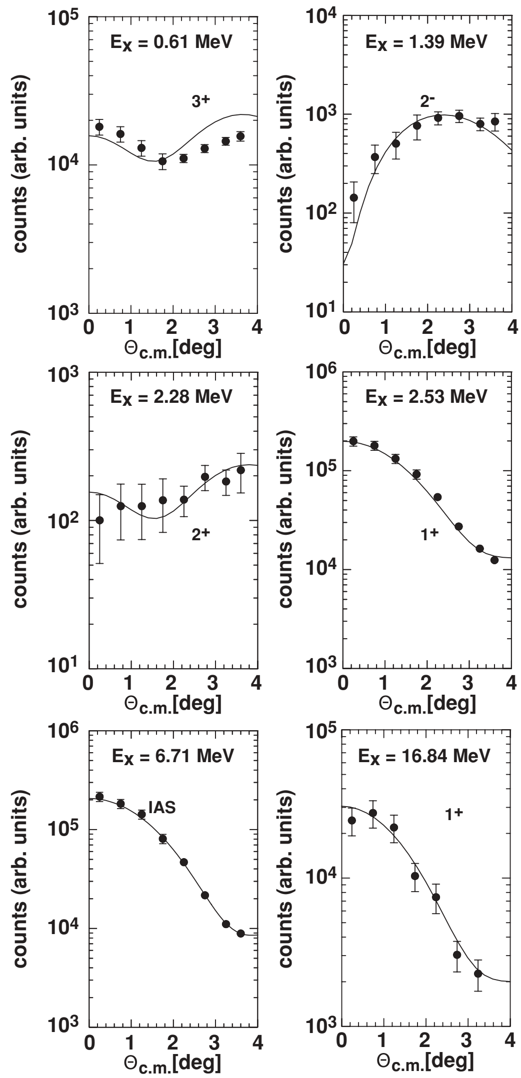

FIG. 3. Angular distributions for the transitions discussed in the text sorted by excitation energy. The solid lines represent DW81 calculations.

B. Determination of Gamow-Teller strength

The existence of a proportionality between the zero-degree cross section of (p, n) and (n, p) charge-exchange reactions and the Gamow-Teller (GT) and Fermi (F) strength was pointed out by Taddeucci *et al.* [5]:

$$\frac{d\sigma(q=0)}{d\Omega} = \left(\frac{\mu}{\pi\hbar^2}\right)^2 \frac{k_f}{k_i} \left\{ \begin{array}{l} N_D^{\sigma\tau} J_{\sigma\tau}^2 B(\mathrm{GT}) \\ N_D^{\tau} J_{\tau}^2 B(F) \end{array} \right. , \qquad (3)$$

where $J_{\sigma\tau}$, respectively, J_τ are the volume integrals of the effective interaction for GT and F transitions. The distortion factors $N_D^{\sigma\tau}$, respectively, N_D^{τ} are ratios between the calculated cross section for distorted and plane waves, which for most cases are taken as equal [5].

More recently, the same relation was also found to be valid in the case of the $(^3\mathrm{He}, t)$ charge-exchange reactions, at least for the light nuclei and for $B(\mathrm{GT})$ values above $B(\mathrm{GT}^-) \approx 0.04$ [23,56–58]. A rather comprehensive discussion about $(^3\mathrm{He}, t)$ reactions at energies above 100 MeV/nucleon and on different nuclei can be found in Ref. [59].

In the present experiment, the large beam dispersion on target disallowed a reliable solid angle acceptance determination and thereby absolute cross sections could not be extracted from the data. Instead, an alternative method was used that employs a GT unit cross section ($\hat{\sigma}_{\mathrm{GT}}$) through which experimental $B(\mathrm{GT}^-)$ values can be evaluated.

If there is a proportionality relation between the GT, respectively, F strength and the $(^3\mathrm{He}, t)$ cross section, the quantity:

$$R^2(E_p, A) = \frac{\hat{\sigma}_{\mathrm{GT}}}{\hat{\sigma}_F} = \frac{\sigma_{\mathrm{GT}}(q \to 0)}{B(\mathrm{GT}^-)} \Big/ \frac{\sigma_F(q \to 0)}{B(F)} \qquad (4)$$

is constant. In the case of a (p, n) reaction at a given incident proton energy E_p, this ratio can be determined as $R^2 = (E_p/E_0)^2$ [5] with $E_0 = 55 \pm 1.7$ MeV. Adopting this relation also for the $(^3\mathrm{He}, t)$ reaction leads to $R^2 = 6.5 \pm 0.4$ at an incident energy of 420 MeV (equivalent to 140 MeV/nucleon for E_p), which is the value used in the present analysis. As the Fermi strength is concentrated in the IAS with a total strength for ^{48}Ca of $B(F) = (N - Z) = 8$, the calculation of $B(\mathrm{GT})$ values is straightforward. The present R^2 value is motivated by keeping consistency with the $B(\mathrm{GT})$ values extracted from the (p, n) measurements [15,19]. In Refs. [11,12] R^2 values for masses near $A = 48$ have been deduced in a different way using only $(^3\mathrm{He}, t)$ data and the various β-decay branches, and more recently, Adachi *et al.* [60] have obtained R^2 values for various nuclei. Given the quoted error margin of these studies, and thinking of the other ambiguities in deriving the $2\nu\beta\beta$-decay half-life, we use the present value of $R^2 = 6.5$.

Following the above quoted procedure, the extracted GT strengths values are listed in Table I. One may note, however, that for some (mostly weak) transitions showing "contamination" from underlying higher J^π transitions, a multipole decomposition was performed before evaluating the GT strength. In those cases an increased statistical error was associated with the extracted $B(\mathrm{GT})$ values (given in Table I) due to the uncertainty in determining this non-GT contribution. We took the approach of adding 50% of the contaminating cross section to the statistical uncertainty of the GT strength and another 25% is estimated as a systematic error.

C. Comparison with (p, n) measurements

To assess the selective power of the $(^3\mathrm{He}, t)$ reaction compared to the elementary (p, n) reaction, it may be instructive to compare the present data taken at 140 MeV/nucleon with the (p, n) data measured at IUCF at 134 MeV [19]. For this purpose the $(^3\mathrm{He}, t)$ spectrum shown in Fig. 2 was folded with a 360-keV resolution function to match the resolution of the (p, n) spectrum. The result is shown in Fig. 4. We note that due to the different Q values and the different masses involved in these two reactions, the momentum transfers are different, requiring for the GT and the F transitions a slight adjustment of the relative strengths as a function of the excitation energy. This adjustment is included in the present comparison. Of course, the momentum dependence of higher multipole transitions

TABLE I. Table of all extracted GT$^-$ values. The contributions originating from higher multipoles as $J^\pi = 2^+$ or 3^+ have been subtracted to deduce the GT$^-$ strength. The errors are statistical errors only with an additional error to take the contribution of higher multipoles into account (see text). The systematic error was estimated to be 25%.

E_x MeV	Contributions from higher multipoles	$B(\text{GT}^-)$
2.53	None	1.09 ± 0.01
2.98	10% of $J^\pi = (2,3)^+$	0.002 ± 0.001
3.07	10% of $J^\pi = (2,3)^+$	0.059 ± 0.004
3.16	None	0.021 ± 0.001
3.72	None	0.100 ± 0.002
3.82	None	0.004 ± 0.001
4.04	20% of $J^\pi = 2^+$	0.010 ± 0.001
4.19	10% of $J^\pi = (2,3)^+$	0.042 ± 0.003
4.33	$J^\pi = 2^-$ [a]	0.021 ± 0.001
4.79	None	0.090 ± 0.004
5.05, 5.11 }	20% of $J^\pi = (2,3)^+$	0.043 ± 0.007
5.23	20% of $J^\pi = 2^+$	0.075 ± 0.007
5.29, 5.36 }	40% of $J^\pi = (2,3)^+$	0.033 ± 0.007
5.44	20% of $J^\pi = 2^+$	0.027 ± 0.002
5.52	15% of $J^\pi = 2^+$	0.066 ± 0.006
5.76	None	0.081 ± 0.004
5.90, 5.96, 6.02 }	30% of $J^\pi = (2,3)^+$	0.118 ± 0.011
6.25	None	0.139 ± 0.009
6.40	20% of $J^\pi = 2^+$	0.031 ± 0.004
6.46	5% of $J^\pi = 2^+$	0.071 ± 0.004
6.62	None	0.214 ± 0.003
Σ		$2.34^{\pm 0.02\,\text{stat.}}_{\pm 0.59\,\text{syst.}}$

[a] $J^\pi = 2^-$ contributions are negligible at 0°.

TABLE II. $B(\text{GT})$ values extracted from (^{3}He, t) and (p,n) reactions on ^{48}Ca. The extraction was done by employing the relation $\hat{\sigma}_{\text{GT}}/\hat{\sigma}_F = (E_p/E_0)^2$ [5] with $E_0 = (55 \pm 1.7)$ MeV. Note that the (p,n) results as presented in Ref. [15] have been slightly rescaled (cf. text). Excitation energies are given in MeV.

GT$^-$ from (^{3}He, t)		GT$^-$ from (p,n)	
E_x	$B(\text{GT}^-)$	E_x	$B(\text{GT}^-)$
2.53	1.09 ± 0.01	2.54	1.16 ± 0.14
3.07	0.059 ± 0.004	3.02[a]	0.043 ± 0.02
3.16	0.021 ± 0.001	3.17[a]	0.061 ± 0.02
3.72, 3.82 }	0.104 ± 0.002	3.69	0.099 ± 0.04
4.19	0.042 ± 0.003	4.14	0.028 ± 0.01
4.79	0.090 ± 0.004	4.79	0.072 ± 0.03
Σ	$1.40 \pm 0.01^{\text{stat.}} \pm 0.35^{\text{syst.}}$		1.46 ± 0.26

[a] The energy resolution of about 360 keV makes the individual $B(\text{GT})$ assignment for these two levels not particularly reliable, and one should rather compare the summed strength with the one from the (^{3}He, t) reaction.

is opposite to GT transitions and cannot be corrected at the same time. This fact is apparent for the lowest 3^+ transition at 0.61 MeV. Here, the larger momentum transfer is connected with the (^{3}He, t) reaction, which results in a slightly stronger excitation. Likewise, due to the higher incident energy in the (^{3}He, t) experiment, the IAS is more strongly excited than in the (p,n) case. This was considered through a 10% reduction of the IAS cross section in the folded spectrum [cf. Eq. (4)]. After taking these important, yet trivial effects into account, the similarity of the two spectra up to about 8 MeV excitation is striking. A sole exception is the IAS transition, which is still about 10% stronger in the (^{3}He, t) reaction than in the (p,n) case, even after taking the above-mentioned energy and momentum-transfer corrections into account. The reason for this is unclear.

The $B(\text{GT}^-)$ values evaluated for single transitions are given in Table II. In the first column, the $B(\text{GT})$ values are those deduced from the present (^{3}He, t) reaction and in the second column those from the (p,n) reaction. The values were calculated using Eq. (4), where for the (p,n) case $R^2 = 5.9 \pm 0.2$ and for the (^{3}He, t) case $R^2 = 6.5 \pm 0.4$. Further, the $B(\text{GT}^-)$ values from the (p,n) experiment have been re-evaluated and differ from the central values derived by Rakers *et al.* [15] by about 12%. Rakers *et al.* [15] and Anderson *et al.* [19] have assumed some background under the IAS, which in view of the present high-resolution (^{3}He, t) results seems to be slightly overestimated. One may also note that for those states that are poorly separated and overlapping in the case of the (p,n) reaction one should rather take the summed values in Table II when comparing them with the (^{3}He, t) reaction.

The total GT$^-$ strength summed for energies up to about 5 MeV is $\Sigma[B(\text{GT})] = 1.40 \pm 0.36$ in the (^{3}He, t) case and $\Sigma[B(\text{GT})] = 1.46 \pm 0.26$ in the (p,n) case.

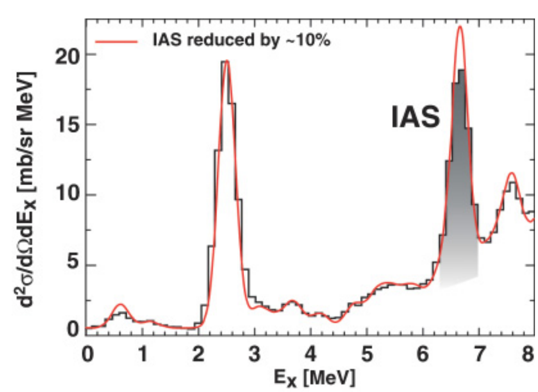

FIG. 4. (Color online) Overlay of the ^{48}Ca(^{3}He, t) spectrum at 140 MeV/nucleon and the ^{48}Ca(p,n) spectrum at 134 MeV [19]. The histogram shows the (p,n) data and the solid line the spectrum from Fig. 5 folded with a resolution function of 360 keV to match the resolution of the (p,n) spectrum. The (^{3}He, t) strength of the IAS was reduced by 10% to take the higher incident energy into account but still exceeds the (p,n) cross section by ≈ 10%.

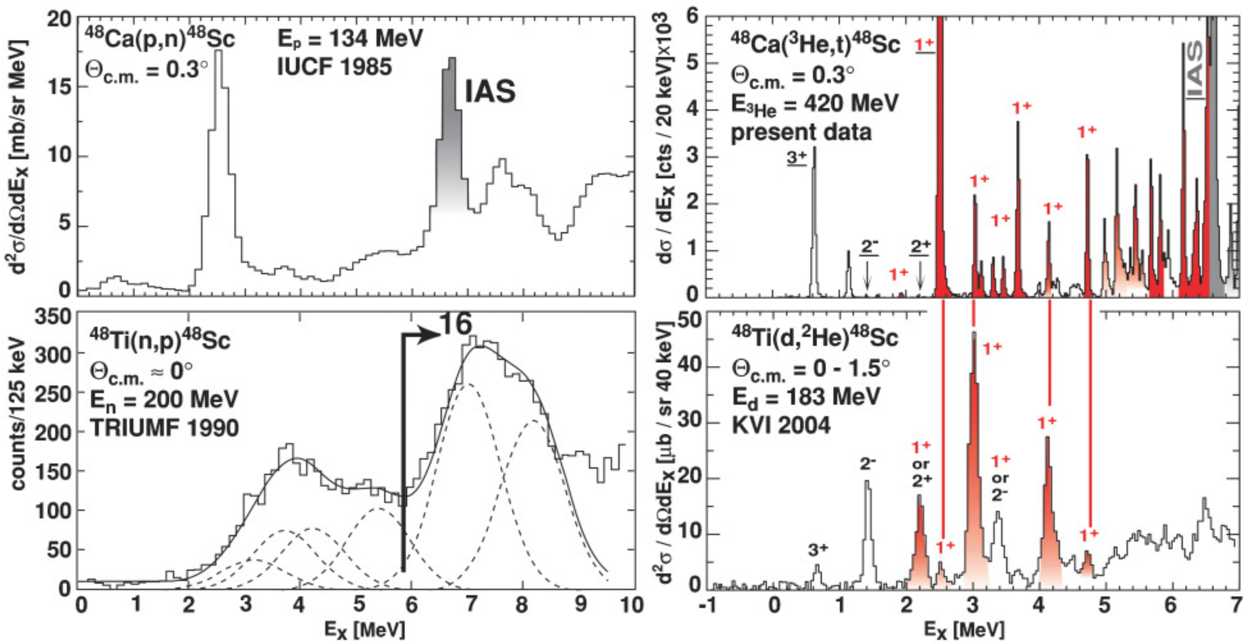

FIG. 5. (Color online) Excitation spectra from the (p, n)-type reactions on ^{48}Ca (upper panel) and (n, p)-type reactions on ^{48}Ti experiments (lower panel). Data were taken from Refs. [3,15,19]. Levels excited in (^{3}He, t) and (d, ^{2}He) are connected by the vertical lines. For states in the (^{3}He, t) spectrum that are underlined, we show angular distributions in Fig. 3.

IV. APPLICATIONS TO DOUBLE BETA DECAY

The importance of combining the charge-exchange reactions in the (p, n) and the (n, p) direction for evaluating nuclear $\beta\beta$-decay matrix elements was already recognized by Alford *et al.* [3] at TRIUMF, who performed the ^{48}Ti(n, p) measurements. However, those (n, p) experiments made use of secondary neutron beams and, therefore, suffered from an inherently poor energy resolution. At the same time, rather thick, isotopically enriched targets were required, which in the case of ^{48}Ti were not readily available as metallic foils. The use of an alternative $^{48}TiO_2$ target, however, produced a rather severe contamination of the oxygen component in the (n, p) spectrum. Nevertheless, by combining the (n, p) results with the (p, n) results from Anderson *et al.* [19], Alford *et al.* [3] were able to deduce a ^{48}Ca $2\nu\beta\beta$-decay half-life of $T_{1/2}^{(2\nu)} = 7.5 \times 10^{18}$ a. The $(d, {}^2\mathrm{He})$ alternative reaction to (n, p) was recently employed by Rakers *et al.* [15] on ^{48}Ti with a significantly better resolution. Combining these new data with the (p, n) data gave a half-life $T_{1/2}^{(2\nu)} = (2.87 \pm 0.51) \times 10^{19}$ a. The enhanced resolution further elucidated details of the underlying nuclear structure, as it was shown that strong transitions in (p, n) direction were correlated with weak transitions in (n, p) direction and vice versa [15].

In Fig. 5 we show all relevant charge-exchange reactions performed so far on ^{48}Ca, indicating the progress made over time in terms of resolution. Clearly, the anticorrelation of the various transition strengths, which was already observed by Rakers *et al.* [15], is confirmed. Combining the $(d, {}^2\mathrm{He})$ data with the present $({}^3\mathrm{He}, t)$ measurement at excitation energies below 5 MeV and adding all individual $\beta\beta$ matrix elements gives $M_{\mathrm{DGT}}^{(2\nu)} = (0.083 \pm 0.016)\mathrm{MeV}^{-1}$ (see Table III). With the phase-space factor [cf. Eq. (1)] $G^{2\nu}(Q, Z) = 1.1 \times 10^{-17}\mathrm{a}^{-1}(\mathrm{MeV})^2$ [61,62] the half-life can be evaluated to $T_{1/2}^{(2\nu)} = (1.32 \pm 0.35) \times 10^{19}$ a. For the summation of the matrix elements one takes the naive assumption that all matrix elements add constructively. Most shell-model

TABLE III. Experimental matrix elements for the ^{48}Ca $2\nu\beta\beta$ decay. The errors quoted are the combined statistical and systematic errors. The levels marked with a dagger (†) are those that may contribute destructively to $M_{\mathrm{DGT}}^{(2\nu)}$ as suggested by most shell-model calculations (cf. text). Energies are given in MeV and matrix elements in MeV^{-1}.

GT$^+$ from $(d, {}^2\mathrm{He})$		GT$^-$ from $({}^3\mathrm{He}, t)$		
E_x	$B(\mathrm{GT}^+)$	E_x	$B(\mathrm{GT}^-)$	$M_{\mathrm{DGT}}^{(2\nu)}(\beta\beta)$
2.20	0.047(2)	–	–	–
2.52	0.014(5)	2.53	1.09(28)	0.028(12)
2.98	0.072(17)	2.98	0.002(1)	0.003(1)†
3.05	0.120(29)	3.07	0.059(20)	0.017(7)†
3.15	0.017(5)	3.16	0.021(6)	0.004(2)†
3.70[a]	0.021(6)	3.72[a]	0.10(3)	0.008(3)
4.00	0.016(5)	4.04[b]	0.010(3)	0.002(1)
4.14	0.090(22)	4.19	0.042(14)	0.010(4)
4.28	0.025(8)	4.33	0.021(6)	0.004(2)
4.76	0.026(8)	4.79	0.090(25)	0.007(3)
Σ	0.45(12)		1.43(38)	0.083(16)

[a]Angular distributions show $J^\pi = 2^-$ contributions, however, at a negligible level at 0°.
[b]Angular distribution of the $(d, {}^2\mathrm{He})$ cross section suggests $J^\pi \neq 1^+$ [15], which is not confirmed by $({}^3\mathrm{He}, t)$.

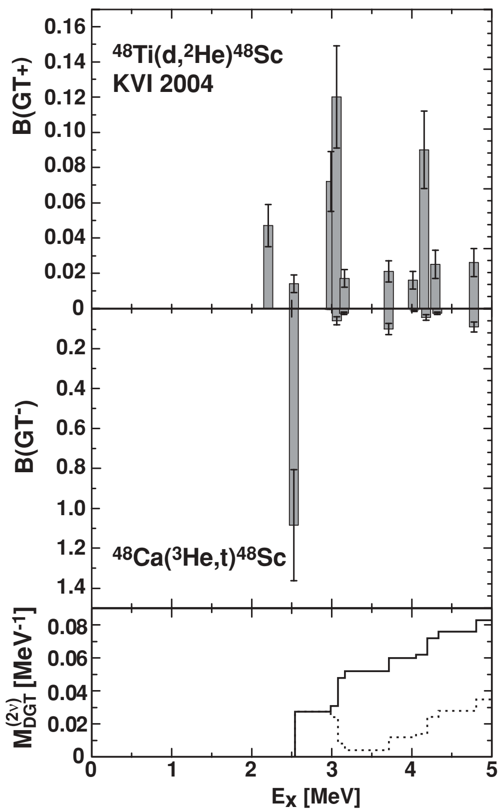

FIG. 6. GT$^{\pm}$ strength deduced from (d, ^{2}He) and (^{3}He, t) experiment (note the different scales). The cumulative sum of the $M_{\mathrm{DGT}}^{(2\nu)}$ is shown in the lower plot, where the levels around 3 MeV were added with different phases (cf. text).

calculations, however, show that any further levels above 5 MeV, which remain experimentally unresolved, would generally contribute destructively [63–65] and, thereby, lower the $M_{\mathrm{DGT}}^{(2\nu)}$ by about 24%. If one applies this reduction to the half-life, as was also done by Rakers *et al.* [15], one arrives at:

$$T_{1/2}^{(2\nu)} = (2.28 \pm 0.60) \times 10^{19} \text{ a},$$

which is consistent with the value given by Rakers *et al.* [15].

As shell-model calculations also almost unanimously predict one single level at 3 MeV contributing destructively [63–65], one can look for the experimentally well-isolated fragments near 3 MeV and try to estimate their contribution to the half-life as a function of the sign of the interference (cf. Tab. III). Figure 6 shows the individual components of the matrix elements and the cumulative sum to the total $M_{\mathrm{DGT}}^{(2\nu)}$ as a function of the interference of the 3-MeV fragments (lower part of Fig. 6). As charge-exchange reactions do not provide information about the sign of the matrix elements, we have taken the approach of quoting the extremes as the likely interval for the true ^{48}Ca $2\nu\beta\beta$-decay half-life:

$$2.4 \times 10^{19} \text{ a} \leqslant T_{1/2}^{(2\nu)} \leqslant 12.9 \times 10^{19} \text{ a}.$$

The result agrees with the results from past counting experiments [66,67] and is in equally good agreement with the recently communicated result from the NEMO-III experiment [68], $T_{1/2}^{(2\nu)} = (3.9 \pm 0.7) \times 10^{19}$ a.

Despite the unknown phases of the various contributing matrix elements, we conclude that the nuclear matrix elements remain an important factor determining the rate of the $\beta\beta$ decay. If one were to take a rather ignorant point of view and assumed the matrix elements to be of order unity, the calculated ^{48}Ca half-life would be in the order of 10^{17} a. In this way one would be in error by about two to three orders of magnitude.

V. CONCLUSIONS

The (p,n)-type charge-exchange reaction (^{3}He, t) on the $\beta\beta$-decay nucleus ^{48}Ca was presented. The measurements were performed at the RCNP facility, Osaka (Japan), with an unprecedented energy resolution of 40 keV. $B(\mathrm{GT}^-)$ values were deduced and compared with previous charge-exchange reaction analysis in (p,n) and (n,p) direction (here also: (d, ^{2}He)), by which the matrix elements for the $2\nu\beta\beta$ decay of ^{48}Ca were evaluated. We have shown that the high resolution is a key element for extracting the matrix elements but also for elucidating details of the nuclear structure.

We have compared the two reaction probes, (p,n) and (^{3}He, t), and after considering trivial momentum- and energy-dependent factors, the (^{3}He, t) reaction and the elementary (p,n) reaction yield identical spectra. However, we want to stress that such a comparison should be made for only the low-momentum transfer region, i.e., preferentially for scattering angles near zero degree. We also feel that caution must still be exercised to conclude that this similarity is a general feature of the two probes. Clearly, this is something that needs to be investigated experimentally, in particular when higher target masses are involved.

ACKNOWLEDGMENTS

We thank the RCNP accelerator staff for their support during the course of the present experiment. We are particularly thankful to B. D. Anderson for providing us with the (p,n) data set. One of us, P.v.B., acknowledges support from DFG under contract number BR799/13-1. We thank H. Baumeister (IKP Münster) for his perseverance in producing a ^{48}Ca target.

[1] B. D. Anderson *et al.*, Phys. Rev. C **36**, 2195 (1987).
[2] B. D. Anderson *et al.*, Phys. Rev. C **43**, 50 (1991).
[3] W. P. Alford *et al.*, Nucl. Phys. **A514**, 49 (1990).
[4] R. Helmer, Can. J. Phys. **65**, 588 (1987).
[5] T. N. Taddeucci *et al.*, Nucl. Phys. **A469**, 125 (1987).
[6] C. D. Goodman *et al.*, Phys. Rev. Lett. **44**, 1755 (1980).
[7] K. P. Jackson *et al.*, Phys. Lett. **B201**, 25 (1988).
[8] S. Rakers *et al.*, Nucl. Instrum. Methods Phys. Res. B **481**, 253 (2002).
[9] S. Rakers *et al.*, Phys. Rev. C **65**, 044323 (2002).
[10] G. W. Hitt *et al.*, Nucl. Instrum. Methods Phys. Res. A **566**, 264 (2006).

[11] T. Adachi *et al*., Phys. Rev. C **73**, 024311 (2006).
[12] Y. Fujita *et al*., Phys. Rev. Lett. **95**, 212501 (2005).
[13] W. C. Haxton and G. J. Stephenson Jr., Prog. Part. Nucl. Phys. **12**, 409 (1984).
[14] M. Doi, T. Kotani, and E. Takasugi, Prog. Theor. Phys. Suppl. **83**, 1 (1985).
[15] S. Rakers *et al*., Phys. Rev. C **70**, 054302 (2004).
[16] S. Rakers *et al*., Phys. Rev. C **71**, 054313 (2005).
[17] H. Ejiri, Phys. Rep. **338**, 265 (2000); J. Phys. Soc. Jpn. **74**, 2101 (2005).
[18] W. P. Alford and B. Spicer, Adv. Nucl. Phys. **24**, 1 (1994).
[19] B. D. Anderson *et al*., Phys. Rev. C **31**, 1161 (1985) and (private communication).
[20] D. Frekers, J. Dilling, and I. Tanihata, Can. J. Phys. **85**, 57 (2007).
[21] R. B. Firestone, V. S. Shirley, C. M. Baglin, J. Zipkin, and S. Y. F. Chu, *Table of Isotopes CD-ROM*, Eighth Edition, Vers. 1.0 (1996).
[22] A. Schulte, T. Ugadawa, F. Osterfeld, and D. Cha, Phys. Lett. **B183**, 243 (1987).
[23] R. G. T. Zegers *et al*., Phys. Rev. C **74**, 024309 (2006).
[24] M. Sasano *et al*., Nucl. Phys. **A788**, 76c (2007).
[25] A. Brockstedt *et al*., Nucl. Phys. **A530**, 571 (1991).
[26] A. Faessler, Prog. Part. Nucl. Phys. **57**, 162 (2006).
[27] S. Elliott and P. Vogel, Annu. Rev. Nucl. Part. Sci. **52**, 115 (2002).
[28] J. Suhonen, Phys. Lett. **B607**, 87 (2005).
[29] H. V. Klapdor-Kleingrothaus, I. V. Krivosheina, A. Dietz, and O. Chkvorets, Phys. Lett. **B586**, 198 (2004); H. V. Klapdor-Kleingrothaus, A. Dietz, I. V. Krivosheina, and O. Chkvorets, Nucl. Instrum. Methods Phys. Res. A **522**, 371 (2004).
[30] R. Arnold *et al*., Phys. Rev. Lett. **95**, 182302 (2005).
[31] H. Ejiri, Prog. Part. Nucl. Phys. **40**, 307 (1998).
[32] C. Arnaboldi *et al*., Nucl. Instrum. Methods Phys. Res. A **518**, 775 (2004).
[33] P. Peiffer, D. Motta, S. Schoenert, and H. Simgen, Nucl. Phys. Proc. Suppl. **B143**, 511 (2005); I. Abt, M. Altmann, A. Bakalyarov, and I. Barabanov, hep-ex/0404039, GERDA proposal submitted to Gran Sasso Scientific Committee.
[34] C. E. Aalseth, D. Anderson, R. Arthur, and F. T. Avignone III, Nucl. Phys. B, Proc. Suppl. **138**, 217 (2005).
[35] K. Zuber, *Summary of Workshop on Nuclear Matrix Elements for Neutrinoless Double-Beta Decay, Institute for Particle Physics Phenomenology*, University of Durham, UK, June 2005 and preprint nucl-ex/0511009; K. Zuber, EPI 2006, Acta Phys. Pol. B **37**, 1905 (2007).
[36] T. Wakasa *et al*., Nucl. Instrum. Methods Phys. Res. A **482**, 79 (2002).
[37] M. Fujiwara *et al*., Nucl. Instrum. Methods Phys. Res. A **422**, 484 (1999).
[38] Y. Fujita *et al*., Nucl. Instrum. Methods Phys. Res. B **126**, 274 (1997).
[39] H. Fujita *et al*., Nucl. Instrum. Methods Phys. Res. B **484**, 17 (2002).
[40] Y. Fujita *et al*., J. Mass Spectrom. Soc. Jpn. **48**, 306 (2000).
[41] H. Fujita *et al*., Nucl. Instrum. Methods Phys. Res. A **469**, 55 (2001).
[42] T. Noro *et al*., RCNP Annual Report (Osaka University, 1991) p. 177.
[43] H. Fujimura *et al*., Phys. Rev. C **69**, 064327 (2004).
[44] W. Steffen *et al*., Phys. Lett. **B95**, 23 (1980).
[45] R. Schaeffer and J. Raynal, program DWBA70 (unpublished).
[46] J. R. Comfort, extendet version DW81 (unpublished).
[47] W. G. Love and M. A. Franey, Phys. Rev. C **24**, 1073 (1981).
[48] M. Rashdan, Eur. Phys. J. A **16**, 371 (2003).
[49] S. Y. van der Werf *et al*., Nucl. Phys. **A496**, 305 (1989).
[50] B. A. Brown *et al*., computer code OXBASH (unpublished).
[51] T. S. Kuo and G. E. Brown, Nucl. Phys. **A114**, 241 (1968).
[52] M. A. Hofstee *et al*., Nucl. Phys. **A588**, 729 (1995); S. Y. van der Werf, computer code NORMOD, KVI Groningen, 1991 (unpublished).
[53] F. Osterfeld, Rev. Mod. Phys. **64**, 491 (1992).
[54] S. Y. van der Werf, Phys. Scr. **T32**, 43 (1990).
[55] J. Kamiya *et al*., Phys. Rev. C **67**, 064612 (2003).
[56] Y. Fujita *et al*., Phys. Rev. C **67**, 064312 (2003).
[57] Y. Fujita *et al*., Phys. Rev. C **66**, 044313 (2002).
[58] Y. Fujita *et al*., Phys. Rev. C **75**, 057305 (2007).
[59] M. Fujiwara *et al*., Nucl. Phys. **A599**, 223c (1996).
[60] T. Adachi *et al*., Nucl. Phys. **A788**, 70c (2007).
[61] T. Tsuboi, K. Muto, and H. Horie, Phys. Lett. **B143**, 293 (1984).
[62] J. Suhonen and O. Civitarese, Phys. Rep. **300**, 123 (1998).
[63] E. Caurier *et al*., Phys. Lett. **B252**, 13 (1990); Erratum in Phys. Rev. C **50**, 225 (1994).
[64] L. Zhao, B. A. Brown, and W. A. Richter, Phys. Rev. C **42**, 1120 (1990).
[65] M. Kortelainen and J. Suhonen, J. Phys. G: Nucl. Part. Phys. **30**, 2003 (2004); M. Kortelainen and J. Suhonen, Phys. At. Nucl. **67**, 1202 (2004).
[66] A. Balysh *et al*., Phys. Rev. Lett. **77**, 5186 (1996).
[67] V. B. Brudanin *et al*., Phys. Lett. **B495**, 63 (2000).
[68] V. Vasiliev, preliminary value communicated during “Physics of Massive Neutrinos,” Blaubeuren, Germany, July 1–5, 2007, Joint Annual Meeting of EU project ILIAS, N4 IDEA, and N6/WP1 ENTApP, organized by A. Fäßler, A. Giuliani, D. Lalanne, and V. Rodin.